Isolated Buildings and the *1997 UBC* Near-Source Factors

John F. Hall, M.EERI, and Keri L. Ryan, M.EERI

Computer simulations are employed to assess the effects of near-source ground motions on base-isolated buildings that meet the provisions of the *1997 Uniform Building Code*. A six-story base-isolated building designed for $N_V = 1.6$ exhibits essentially elastic structural behavior when subjected to six actual ground motions containing strong near-source effects. However, two simulated records, one intended to represent the most severe motions from the 1994 Northridge earthquake and the other a strong motion from a hypothetical $M_w7.0$ thrust earthquake produce larger responses well into the nonlinear range. In addition, a 113 cm ground displacement pulse of three-second duration, which is close to the period of the isolated buildings, causes story drifts of nearly 5% for the $N_V = 1.6$ design and over 2% for a stronger $N_V = 2$ design. Such drifts are effectively reduced when supplemental dampers are added alongside the isolators. The original $N_V = 1.6$ design with supplemental damping in the amount of 20% of critical experiences only 1.3% drift for the same three-second ground displacement pulse.

INTRODUCTION

Near-source factors for base-isolated buildings increased significantly in the *1997 Uniform Building Code (UBC)* (ICBO 1997) compared to 1994 values. This reflects greater understanding of the potential for large, rapid ground displacements in the near-fault region to place severe demands on long-period structures. Accommodating the large code-required displacement capability in the bearings requires they be of considerable size. If rubber isolators are used, the large diameter means they will be stiff, making it harder to achieve the desired degree of isolation, especially with smaller buildings. Supplemental damping alongside the bearings (Hall et al. 1995, Asher et al 1996, Makris and Chang 1998; see Kasalanati and Constantinou, 1999, for an application to bridges) reduces the bearing displacements and, hence, the size of the bearings as well, but some engineers feel that such damping may also reduce the effectiveness of the isolation by exciting higher modes and thereby increase story drifts and accelerations in the superstructure (Kelly 1999). In addition, there is also the question about whether the higher near-source factors in the 1997 Code are even enough to provide the desired degree of protection to the structure. The *1997 UBC* anticipates that superstructures of base-isolated buildings will behave nearly elastically under the design-basis earthquake.

The example considered in this paper is a six-story base-isolated building designed to meet the near-source requirements in the *1997 UBC*. This is accomplished by using large but very soft pads of high-damping rubber and making use of their expected capability for high shear strains (Kelly 1997). The initial designs omit supplemental damping and restraining devices, but stiffening of the rubber under high strain provides some restraint naturally.

(JFH) Division of Engrg. and Applied Science, Caltech, Mail Code 104-44, Pasadena, CA 91125
(KLR) Dept. of Struct. Engrg., Mechanics and Materials, University of California, Berkeley, CA 94720

Effect of supplemental damping is examined in subsequent designs. Special provisions are employed in the frame design to control uplift. Results are presented for actual and simulated ground motion recordings containing strong near-source effects as well as for a suite of simple displacement pulses over which the period of the pulse is varied.

BUILDING DESIGN

The structure is a six-story moment frame (Figure 1) supported on rubber bearings consisting of alternating layers of rubber and thin steel plates. Dead loads are 3.83 *kPa* (80 *psf*) roof, 4.55 *kPa* (95 *psf*) floors 2 to 6, 6.22 *kPa* (130 *psf*) first floor, and 1.68 *kPa* (35 *psf*) cladding, giving a total dead weight W = 31.1 *MN* (7000 *kips*). The design live load is 2.39 *kPa* (50 *psf*). Seismic parameters from the *1997 UBC* are Zone 4, Source A with a fault distance ≤ 2 *km* (the most severe near-source category in the Code), and soil type S_D. Source A is defined as a fault with a high rate of seismic activity (slip rate ≥ 5 *mm* per year) that is capable of producing M ≥ 7.0 earthquakes.

	Exterior Frame		Interior Frame	
	Column	Girder	Column	Girder
1	W14X193	W30X211	*W30X211*	W30X292
2	W14X145	W24X162	*W30X173*	W24X229
3	W14X109	W24X117	*W30X116*	W24X162
4	W30X211	W21X 93	B24/1.50	W21X122
5	W30X173		B24/1.12	
6	W30X116		B24/0.75	

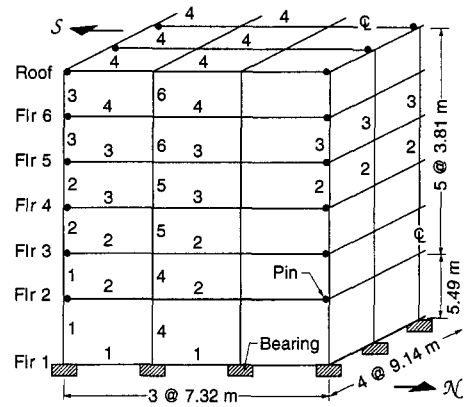

Figure 1. Data for six-story building. B = box with dimensions in inches. Weak axis in italics.

Design of the isolation system opts for squat rubber bearings without supplemental damping or separate restraining devices, as advocated by Kelly (1997,1999). Short bearings and a large design displacement mean high design shear strains, and a usable range in excess of 300% is thought to be practical (Kelly, 1997). Beyond about 200%, stiffening in the rubber provides some natural restraint which is viewed as an advantage. Material damping in the rubber is desirable, and a Code damping factor β_D = 10% of critical can be achieved. This quantification of damping refers to the nominal isolated mode of the building at the design period which is characterized by a rigid structure and flexible isolators.

Selection of the nominal design period T_D as 2.6 seconds produces a design displacement D_D of 68.9 *cm* for the bearings, computed from the Code formula (ICBO, 1997)

$$D_D = (g/4\pi^2)\cdot C_{VD}T_D/B_D, \quad (1)$$

where C_{VD} is a function of the zone, source, fault distance and soil type (computed as $0.64N_V$ where the near-source factor N_V equals 2 for Source A with a fault distance ≤ 2 *km*); B_D = 1.2 is a damping coefficient corresponding to β_D = 10%; and g is the acceleration of gravity. [Under the *1994 UBC* with Zone 4, highest near-field factor N = 1.5, and soil type S_2, the design bearing displacement D_D would have been only 46 *cm*, about 33% smaller than the

newer Code value.] Accounting for torsion and maximum earthquake according to the *1997 UBC* increases the bearing displacement to about 103 *cm* (D_{TM} in the Code), and a stability check is required at this displacement. With these considerations, the bearing diameter Φ_b is taken as 114 *cm*, which makes a large bearing. In a later section of this paper, supplemental damping will be employed to reduce Φ_b.

Other parameters related to bearing design are height of rubber and shear stiffness. To achieve $T_D = 2.6$ seconds, the secant shear modulus of the rubber at displacement D_D is taken as $G_{SEC} = 344$ *kPa* (49.9 *psi*), which is about as low as is currently practical, and this gives a rubber height h_r of 38.1 *cm*. Thus, the design displacement D_D corresponds to a shear strain of 181%, and D_{TM} to a shear strain of 271%. The horizontal secant stiffness of a bearing is

$$K_{SEC} = \pi(D_b/2)^2 \cdot G_{SEC}/h_r = 927 \text{ kN/m } (5.29 \text{ k/in}), \quad (2)$$

which satisfies

$$T_D = 2\pi/(20g \cdot K_{SEC}/W)^{0.5}, \quad (3)$$

where 20 is the number of bearings. Each bearing is fully bonded to the structure and foundation to transfer moment at the top and bottom (not a dowelled connection). This is essential to maintaining stability under high shear strains. All 20 bearings are taken to be identical.

The base shear V_S for superstructure design is the force carried by all bearings at displacement D_D, divided by the reduction factor $R_I = 2$. Thus, $V_S = 20 \cdot K_{SEC} \cdot D_D/2 = 6.39$ *MN* (1436 *kips*), which gives a design base-shear coefficient V_S/W of 0.205. Design of the superstructure is considered for gravity loads and for lateral seismic loads only in the direction of the short dimension (N-S) of the building. Torsion is included by an increase in V_S of 6%. The seismic design is actually controlled by the story drift limit of 0.5%, which means that extra strength above the Code base shear value will be present. A primary consideration, evident under dynamic analysis, is handling uplift (Ryan and Hall, 1998). In this regard, in order to distribute more of the overturning to interior columns, all five N-S frames are designed as moment frames; exterior frames on the east and west faces are made about two-thirds as stiff as each of the three interior ones; and simple beam connections are used at the northern and sourthernmost columns from floor 2 to the roof. Beams and columns are of A36 steel. Computations were carried out by static planar analysis of the N-S frames coupled together with rigid diaphragms, and the completed design is shown in Figure 1.

A second version of the six-story building is designed according to the next near-source category in the Code below the one considered above: either Source A with a fault distance between 2 *km* and 5 *km* or Source B with a fault distance ≤ 2 *km*. For both cases, $N_V = 1.6$ leading to $C_{VD} = 1.02$, a reduction of 20%. Source B covers the faults between Sources A and C, the latter defined as a fault with slip rate ≤ 2 *mm* per year which can produce only $M < 6.5$ earthquakes. Keeping the same period $T_D = 2.6$ seconds and damping $\beta_D = 10\%$ lowers the design bearing displacement D_D by 20% to 55.2 *cm*. This same percentage is used to reduce the bearing diameter Φ_b to 91.4 *cm*, to reduce the height of rubber h_r to 30.5 *cm*, and to increase the rubber modulus to $G_{SEC} = 430$ *kPa* (62.4 *psi*), which produces the same value as before for the horizontal secant stiffness K_{SEC} of the bearing. Shear strains corresponding to D_D and D_{TM} are still 181% and 271%, respectively. The design base shear V_S drops by 20% to 5.11 *MN* (1149 *kips*), giving a design base-shear coefficient $V_S/W = 0.164$. Instead of redesigning the frames, the original beams and columns are scaled down by 20% in their cross-sectional area, moment of inertia and plastic section modulus. This allows comparison on a consistent basis.

The two buildings will be denoted by B100(0) for the original design (N_V = 2) and B80(0) for the design for the less severe near-source category (N_V = 1.6). The notation refers to the relative strength of the structure (100% or 80%) and, to be consistent with later notation, the amount of supplemental damping (in parentheses) which is added alongside the isolators.

The superstructures of both buildings B100(0) and B80(0) meet or exceed the fixed-base building requirements in the *1997 UBC* for similar design parameters, owing to different design objectives in the Code. A fixed-base design is expected to yield considerably under the design-basis earthquake. However, an isolated design is expected to remain nearly elastic, as indicated by the R_I of 2 which is essentially an over-strength factor.

MODEL FOR DYNAMIC ANALYSIS

The five N-S frames are modelled as planar beam-column frames with rigid diaphragm coupling; P-Δ effects are included; and yielding is represented by plastic hinging when the moment at the end of a beam or column reaches the plastic moment strength of the member. The yield strength of steel is taken as 290 *MPa* (42 *psi*), 17% higher than the nominal value. Center-to-center dimensions of the frame members are used without panel zone flexibility. Gravity loads include the dead weight and a reduced 0.72 *kPa* (15 *psf*) live load, and they are applied first followed by the horizontal component of ground motion. Foundation is assumed rigid. Some live load is included in the building mass: 0.48 *kPa* (10 *psf*) for horizontal degrees of freedom and 0.72 *kPa* (15 *psf*) for vertical degrees of freedom. Viscous damping is provided by dashpots that resist interstory horizontal velocities. The force carried by all the dashpots in a story is capped at a level equal to the story shear force produced by lateral design forces corresponding to base-shear coefficients V_S/W = 0.02 and 0.016 for buildings B100(0) and B80(0), respectively. This cap is reached at an interstory velocity of 25.4 *cm/sec* for B100(0) and 22.7 *cm/sec* for B80(0), the latter having been scaled by $.8^{0.5}$ to keep the same fraction of critical damping in the linear range. The reason for capping the damping forces is to keep them from getting unrealistically large compared to the forces carried by the yielding frame.

Each column is supported by a rubber bearing with a nonlinear horizontal force-deflection relation (F_b vs. d_b; see Figure 2) which is bilinear up to a shear strain of 200% and stiffens beyond. A ratio α of secondary to primary stiffness of 0.3 is used for the bilinear part, and the primary stiffness is K_P = 2555 *kN/m* (14.6 *kips/in*). This gives period T_D = 2.6 seconds and damping β_D = 10% of critical for a cycle at D_D. The equation for the stiffening part of the horizontal force-deflection relation for $d_b \geq d_{bs}$ is

$$F_b = F_{bs} + K_\infty \cdot (d_b - d_{bs} - Q_\infty) + K_\infty Q_\infty \cdot exp[(\alpha K_P/K_\infty - 1)(d_b - d_{bs})/Q_\infty], \quad (4)$$

where $d_{bs} = 2h_r$ is the bearing displacement at initiation of stiffening, F_{bs} is the bearing force at initiation of stiffening, and K_∞ and Q_∞ are asymptotes of K and Q (see Figure 2) as $d_b \rightarrow \infty$. The latter are chosen as $K_\infty = 1.25\ K_P$, and Q_∞ = 17.8 *cm* and 14.2 *cm* for buildings B100(0) and B80(0), respectively. The relation in Figure 2 is plotted to scale for building B100(0). The one for building B80(0) would appear shifted down by 20% and to the left by 20%.

In the vertical direction, linearity of a bearing is assumed with a stiffness K_V = 1250 *MN/m* (7141 *kips/in*), a high value characteristic of multi-layered bearings. This vertical stiffness is used for both compression and tension and is not considered to depend on lateral displacement.

The moment which develops in a bearing as it shears is included in the analysis as a moment load applied to the structure joint at the top of the bearing. This moment M_b, shown

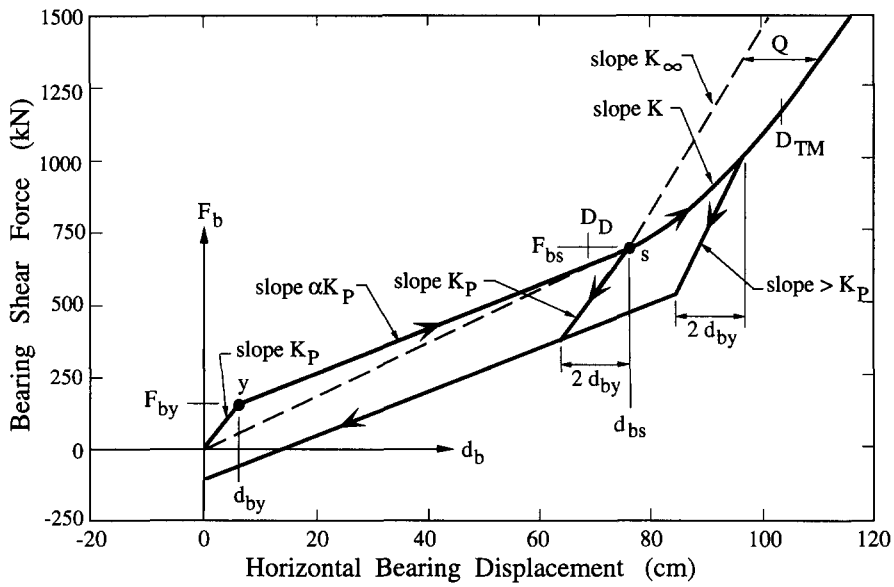

Figure 2. Horizontal force-deflection relation (F_b vs. d_b) for a rubber bearing. Left half (not shown) is similar. Curve shown applies for building B100(0).

below in Figure 3, is related to the dynamic axial compressive force P_b and shear force F_b in the bearing by

$$M_b = 0.5 \cdot (P_b d_b + F_b h_b), \tag{5}$$

where h_b = total bearing height including rubber layers and steel plates, taken as 48.3 *cm* for building B100(0) and 40.6 *cm* for building B80(0).

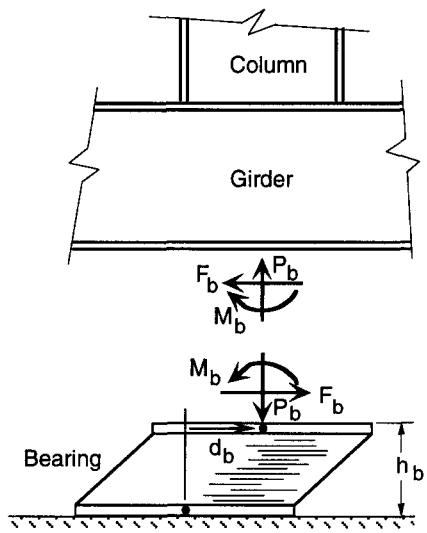

Figure 3. Force and moment transfer between rubber bearing and steel frame (shown separated).

The analytical model produces fundamental periods of the elastic superstructure (fixed base) of 1.03 seconds and 1.15 seconds for buildings B100(0) and B80(0), respectively, computed assuming the bearings are infinitely stiff in horizontal and vertical directions. The computed periods of the isolated buildings, using K_{SEC} and K_V of the bearings, are 2.84 seconds [building B100(0)] and 2.88 seconds [building B80(0)]. Push-over strengths of the superstructures (infinitely stiff and strong bearings) expressed in terms of the dead weight are 0.50W [building B100(0)] and 0.40W [building B80(0)]. The push-over analyses use static lateral loads proportional to the Code design forces over the height of the building. In the dynamic analysis, the constant average acceleration method is employed for time integration with iterations in each time step until convergence is obtained.

DESIGNS WITH SUPPLEMENTAL ISOLATOR DAMPING

The factor B_D in the Code formula for D_D can include contributions from sources of damping in addition to that inherent to rubber. A larger B_D reduces D_D, allowing a bearing with smaller diameter to be used and facilitating the design of elements that cross the isolation interface. For these reasons, supplemental damping often been used in practice (Asher et al., 1996, for example).

To consider this design option, viscous dampers are placed alongside the rubber bearings to increase the damping β_D from 10% of critical to 20% of critical. This gives $B_D = 1.5$, and keeping T_D at 2.6 seconds lowers D_D by 20% to 55.2 *cm* for $N_V = 2$ and 44.1 *cm* for $N_V = 1.6$. Two new isolated buildings are designed with supplemental damping included and are denoted by B80(10) for $N_V = 2$ and B64(10) for $N_V = 1.6$, where the value in parentheses gives the amount of supplemental damping as a percent of critical. Based on the design of the original building B100(0), the factor of 20% is applied to produce $\Phi_b = 91.4$ *cm*, $h_r = 30.5$ *cm* and $G_{SEC} = 430$ *kPa* (62.4 *psi*) for building B80(10); and a further 20% factor results in $\Phi_b = 73.2$ *cm*, $h_r = 24.4$ *cm* and $G_{SEC} = 538$ *kPa* (78.0 *psi*) for building B64(10). Both buildings maintain the same value as before for horizontal secant stiffness K_{SEC} of a bearing. Shear strains corresponding to D_D and D_{TM} are unchanged at 181% and 271%, respectively, and stiffening of the rubber still begins at 200%. The ratio α of secondary to primary stiffness in the bilinear part of the relation remains at 0.3, so the contribution to β_D from the rubber also stays at 10% of critical. In the vertical direction, the same value of K_V is kept. F_b vs. d_b relations for a bearing would be that shown in Figure 2 but shifted down and to the left by 20% for building B80(10) and by 36% (two reductions of 20%) for building B64(10). Superstructure designs are obtained as described earlier by scaling the section properties of the beams and columns. From the original design of building B100(0), the reduction amounts are 20% for building B80(10) and 36% for building B64(10). Capped values for the interstory dampers are appropriately scaled as well. Note that buildings B80(0) and B80(10) are the same except for the supplemental isolation dampers in the latter.

The supplemental dampers are linear, and the total damping constant C for all such added dampers in a building is computed as

$$C = 4\pi \cdot 0.10 \cdot (W/g) / T_D = 1.53 \text{ MN-sec/m } (8.76 \text{ kip-sec/in}). \quad (6)$$

The force F_d carried by a damper would be computed as the product of the damper's individual C value and the relative horizontal velocity between the ground and the 1st floor. Viscous dampers can also be constructed with a nonlinear force-velocity relation (Seleemah and Constantinou, 1997), but this feature is not included here.

GROUND MOTION

Dynamic analyses are conducted for a set of recorded and simulated accelerograms containing strong near-source effects as well as for a suite of simple displacement pulses. The recorded motions include 1978 M_w7.4 Tabas (TAB), 1989 M_w 6.9 Loma Prieta at Los Gatos Presentation Center (LGP), 1992 M_w7.2 Landers at Lucerne Valley (LUC), 1994 M_w6.7 Northridge at Sylmar County Hospital free-field (SYL) and at Rinaldi Receiving Station (RRS), and 1995 M_w6.9 Kobe at Takatori (TAK). Two other records are taken from simulations, one of the Northridge earthquake and one of a hypothetical M_w7.0 earthquake on a blind-thrust fault. These are referred to by their site designations: H06 for Northridge and C05 for the thrust event. Record H06 is intended to represent the most severe motion from the Northridge earthquake, while C05 is one of the stronger motions from the thrust earthquake simulation. All of the above ground motions are horizontal components in the direction of maximum peak-to-peak ground velocity. Another record, the often used N-S component from 1940 M_w6.9 Imperial Valley at El Centro (ELC), scaled amplitude-wise by 1.5, is included as a reference. One final record, component 230° from 1979 M_w6.4 Imperial Valley at Bonds Corner (BCR), has mainly high-frequency components and provides a contrast to the near-source motions. Displacement time histories of all ten ground motions are plotted to the same scale in Figure 4. Pseudo acceleration and displacement response spectra appear in Figure 5. Additional details on most of these ground motions can be found in (Hall, 1997). The geometry of the thrust earthquake simulation is shown in Figure 6.

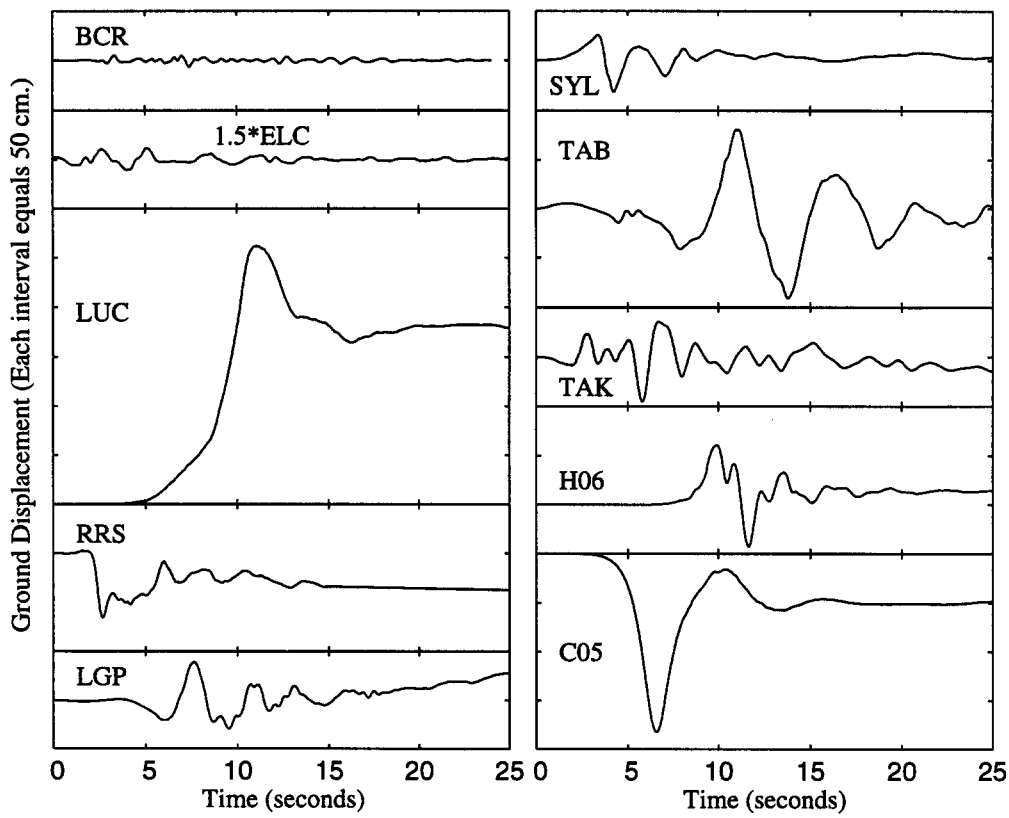

Figure 4. Displacement time histories of the eight actual and two simulated earthquake motions.

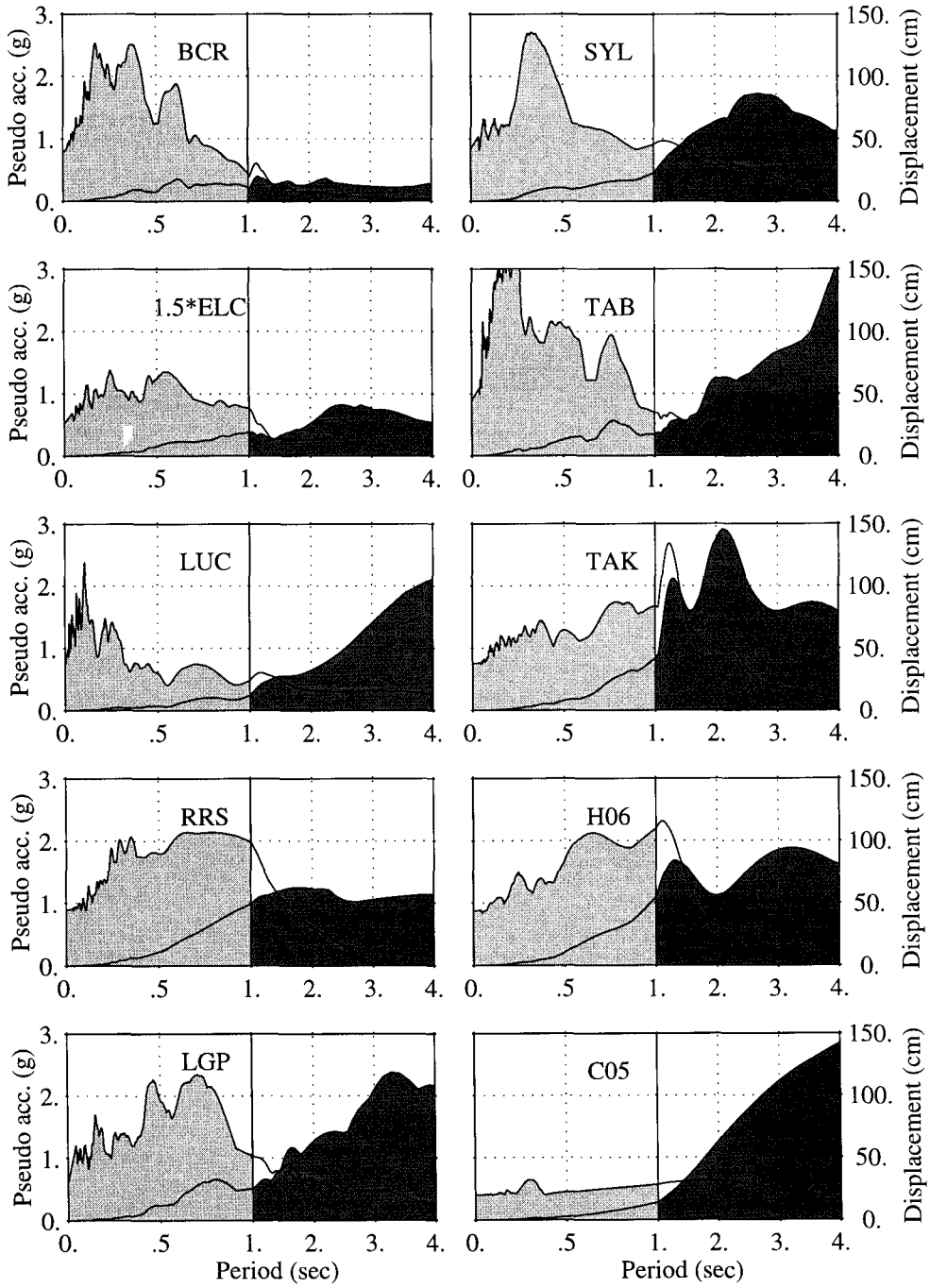

Figure 5. Pseudo acceleration (light gray) and displacement (dark gray) response spectra for the eight actual and two simulated earthquake motions. Damping is 5% of critical.

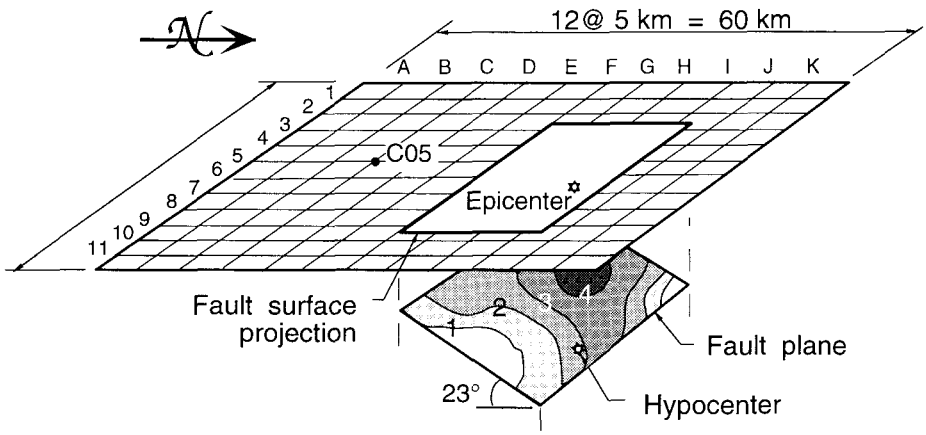

Figure 6. Geometry of the M_w7.0 blind-thrust earthquake simulation showing the dipping fault plane, contours of fault slip in meters, and 121 ground-surface sites where motions are computed (taken from Hall et al., 1995). Site C05 is marked.

Each motion in the suite of simple pulses consists of a forward and back displacement (Figure 7) intended to be characteristic of the fault-normal component of near-source ground motion. Period T_P of the pulse is varied from 0.5 seconds to 5.0 seconds with the peak velocity held constant at 128.6 *cm/sec*, except below $T_P = 1.05$ seconds where the peak acceleration is held constant at 0.80g. This produces a peak displacement increasing from 7 *cm* at $T_P = 0.5$ seconds to 188 *cm* at $T_P = 5.0$ seconds (Figure 8). Magnitudes of the earthquakes which could create such motions would be greater for the larger displacements. The pulse at $T_P = 4.5$ seconds has similar characteristics to the C05 simulated motion.

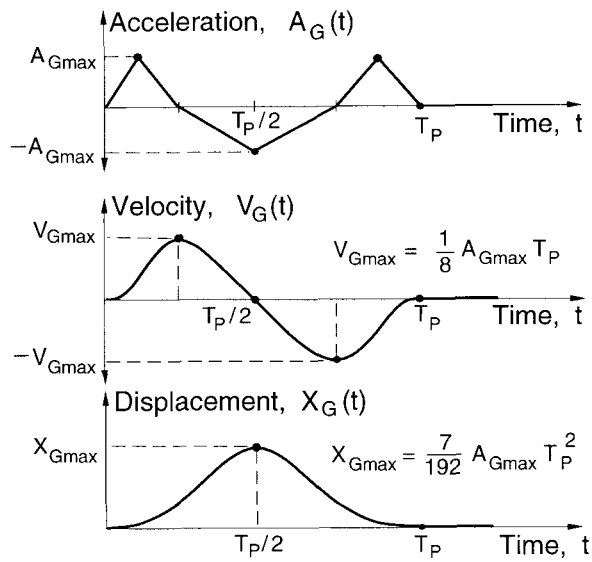

Figure 7. Simple displacement pulse time history, also showing acceleration and velocity histories.

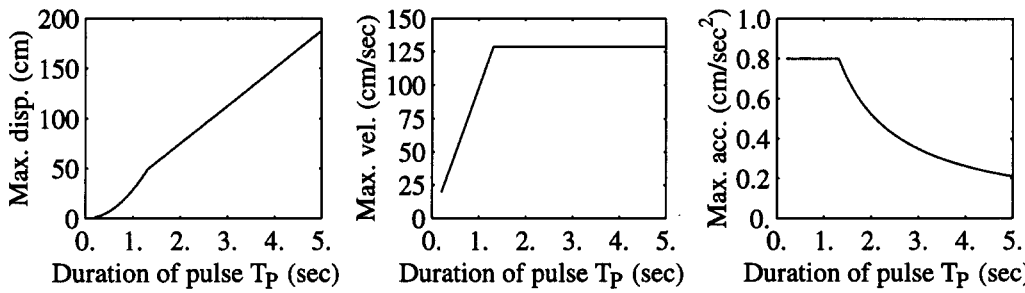

Figure 8. Maximum values of displacement, velocity and acceleration for the simple displacement pulse of Figure 7, shown as a function of pulse duration T_P.

RESULTS

Earthquake responses are computed for all four isolated buildings: B100(0), B80(0), B80(10) and B64(10). Results for the set of recorded and simulated motions are shown in Figure 9 for peak values of horizontal bearing displacement d_b, story drift γ, total shear force $\mathcal{F}_b$ in the bearings ($\mathcal{F}_b = 20 \cdot F_b$), plastic hinge rotation θ_P at the end of a beam or column at any floor above the 1st floor, horizontal acceleration A_r of the roof, and uplift tensile stress σ_b in a bearing. The ten earthquake records are listed according to increasing isolator displacement for building B100(0). In this order, the eight actual records precede the two simulations.

Maximum isolator displacements d_b for B100(0) and B80(0) correspond fairly well to the spectral displacement values in Figure 5 at the 2.6-second period, which vary considerably from record to record. Some of the isolator displacements are well past the 200% shear strain level where the rubber begins to stiffen. The simulated record C05 produces the largest isolator displacement of 93 *cm* for building B100(0) and the largest rubber shear strain of 283% for building B80(0), the latter slightly exceeding the strain at D_{TM}. Records LUC and TAB, which are from the two biggest earthquakes, are less severe at the 2.6-second period than some of the other records, and so produce smaller isolator displacements, but they would have greater effect at longer periods. Addition of supplemental damping [buildings B80(10) and B64(10)] reduces the isolator displacements significantly.

As seen in Figure 9, the isolation systems for both buildings B100(0) and B80(0) are effective in limiting story drifts γ to about 1% or less for the eight actual earthquake records, with the performance of building B100(0) being somewhat better. For the simulated records H06 and C05, larger story drift occurs, especially that for building B80(0) which reaches 3.4% under C05, compared to 1.4% for B100(0). These much higher drifts for building B80(0) are due to its being 20% weaker than B100(0) and also because stiffening in the isolators of building B80(0) increases its base shear force ($\mathcal{F}_b$ in Figure 9) to about 66% of the building dead weight. Under records H06 and C05, even though the isolators of building B80(0) displace less than those of B100(0), they end up transmitting more force into the building because stiffening starts at 61 *cm* for building B80(0) compared to 76 *cm* for B100(0).

The alternate designs with supplemental damping experience slightly higher story drifts than those of the original buildings [B80(10) vs. B100(0); B64(10) vs. B80(0)]. This can be attributed to their weaker designs [B80(10) being 20% weaker than B100(0); B64(10) being

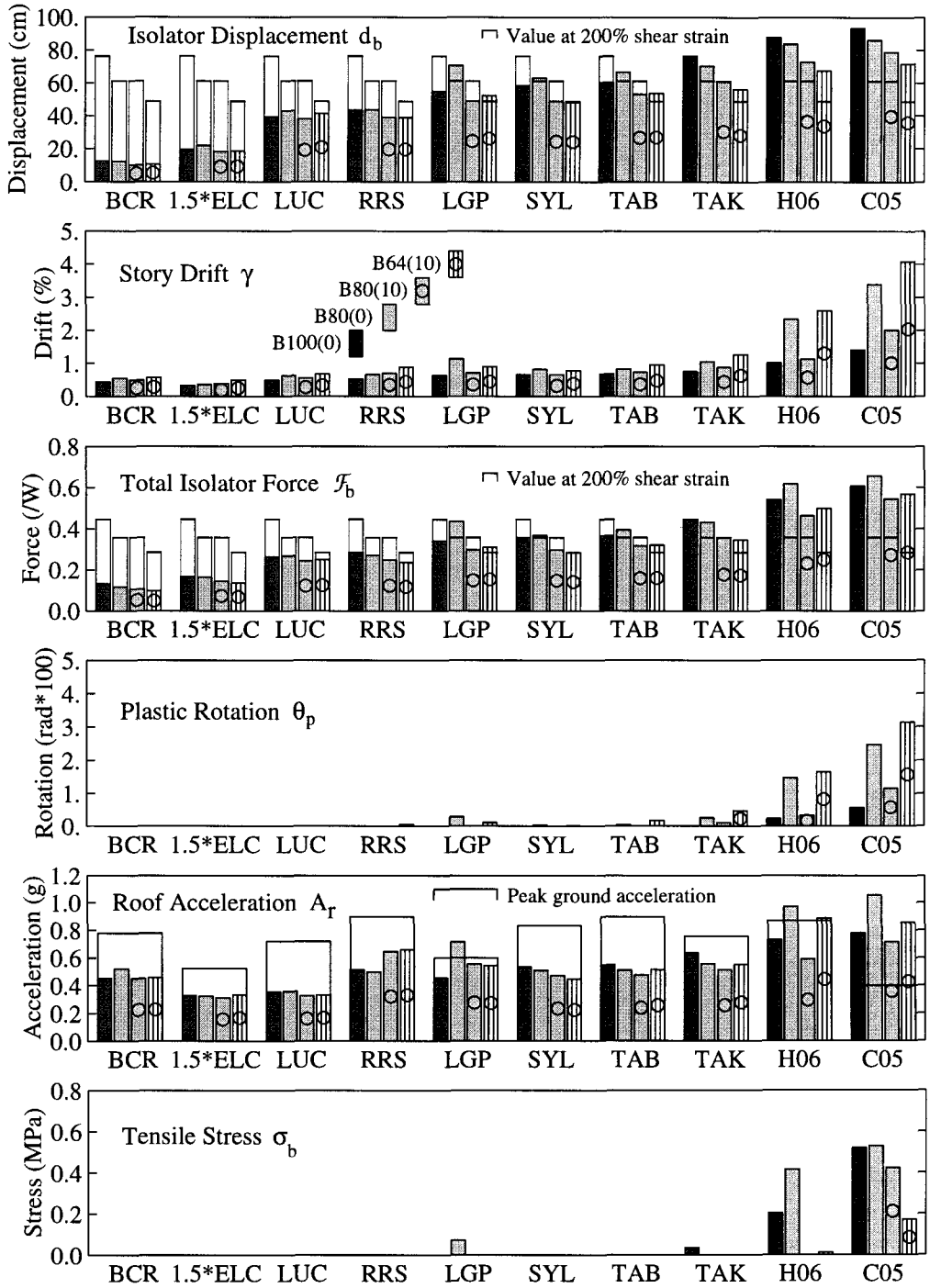

Figure 9. Peak responses of B100(0), B80(0), B80(10) and B64(10) to ten earthquake records.

20% weaker than B80(0)] and not to any adverse effects of supplemental damping, as can be seen in a comparison of buildings B80(0) and B80(10) which are identical except for the presence of 10% supplemental damping in the latter. For these two buildings, addition of supplemental damping reduces story drift for most of the records, often by a significant amount. This observation, which is at odds with the views expressed by Kelly (1999), is examined further in the next section.

Amount of plastic rotation θ_p (Figure 9) in units of percent (radians × 100) is about one percent less than the amount of story drift, and so the structural responses to the eight actual records are either elastic or essentially elastic. Only under the simulated H06 and C05 records for buildings B80(0) and B64(10), the two N_V=1.6 designs, do the plastic rotations reach the 0.02 to 0.03 radian range. These rotations indicate significant yielding but are not beyond what a well designed and constructed steel frame should be able to withstand.

The roof acceleration data A_r in Figure 9, which indicate potential for damage to a building's contents, show that significant acceleration can occur in the structure, although the accelerations at lower floors would be somewhat smaller. Peak accelerations at the roof are below those of the ground in most cases. For example, the 0.83g ground acceleration in the SYL record is deamplified to 0.53g at the roof of building B100(0). Roof accelerations are higher for the simulated records H06 and C05, about 1g for building B80(0), and for C05 the roof motion shows considerable amplification over the moderate ground acceleration.

The final response parameter in Figure 9, uplift tensile stress σ_b, is eliminated entirely for most of the cases under the eight actual records, and it is only really apparent for the simulated records H06 and C05. The highest tensile stress in an isolator is about 0.53 *MPa* for building B80(0) under C05. Although there is not much full scale test data on the tensile capacity of rubber bearings, especially under large simultaneous shear strain, this amount of tension does not seem excessive.

Various time histories of building B80(0) under simulated record H06 are shown in Figure 10: horizontal displacements of the ground as well as floors 1 and 2 plus the roof, shear and vertical stresses in the corner bearing on the north side of the building (where the largest tensile stress occurs), and horizontal acceleration of the roof. The floor motions show that most of the deformation takes place across the bearings (difference between ground and 1st floor motion), although, as mentioned above, the story drifts are past yield. The maximum bearing displacement occurs at 12.2 seconds during the largest swing of the building, and it reaches 84 *cm* which is well into the stiffening range of the rubber. This stiffening is the reason for the sharpened peak in the shear stress history of the bearing at the same time. The large lateral force associated with this peak propagates up the building and causes the 0.97g peak acceleration at the roof. The only tensile excursion in the bearing also occurs during the swing of the building at 12.2 seconds.

Shown in Figure 11 are results for the suite of simple pulses computed for pulse durations T_P from 0.5 to 5.0 seconds at an increment of 0.5 seconds. Included are peak values of isolator displacement d_b, story drift γ and uplift tensile stress σ_b in a bearing. Relative values among the four buildings are similar to what was observed from the earthquake records. However, some of the pulses, especially T_P = 3 and 3.5 seconds, produce isolator displacements and story drifts greater than those of any of the earthquake records, actual or simulated, including C05 whose pulse duration of about 4.5 seconds puts it beyond the range of the largest responses. The maximum of the peak isolator displacements is 107 *cm* for building B100(0), while the

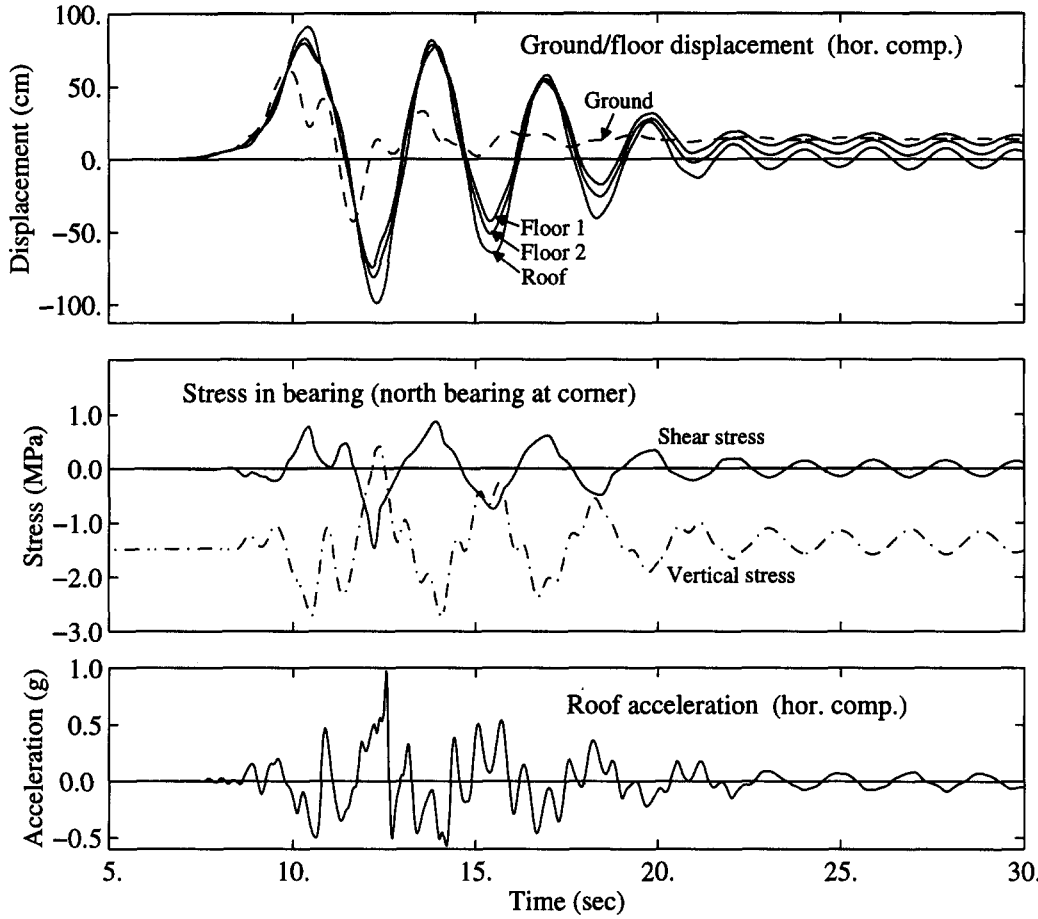

Figure 10. Various response time histories for building B80(0) under the simulated record H06.

largest story drifts are in the range of 2% to slightly above 3% for buildings B100(0) and B80(10), the two N_V=2 designs, and are well above 4% for buildings B80(0) and B64(10), the two N_V=1.6 designs. Uplift tensile stress in a bearing is still well controlled with the maximum value reaching 0.70 *MPa*. The ability of a pulse of T_P = 3 or 3.5 seconds to produce large response is due to its match with the period of the isolated building when vibrating in the large amplitude range.

Time histories for horizontal displacement of the ground, floors 1 and 2, and the roof are plotted in Figure 12 for the simple pulse of T_P = 3 seconds. With this duration, the ground reaches its maximum displacement of 113 *cm* and begins to reverse just as the fast moving building is catching up to the ground and passing it in the forward direction. What follows are large deformations in the bearings and superstructure. This mechanism, which is less critical for both shorter and longer pulses, is also seen to be partially responsible for the large swing of the building under record H06 (Figure 10).

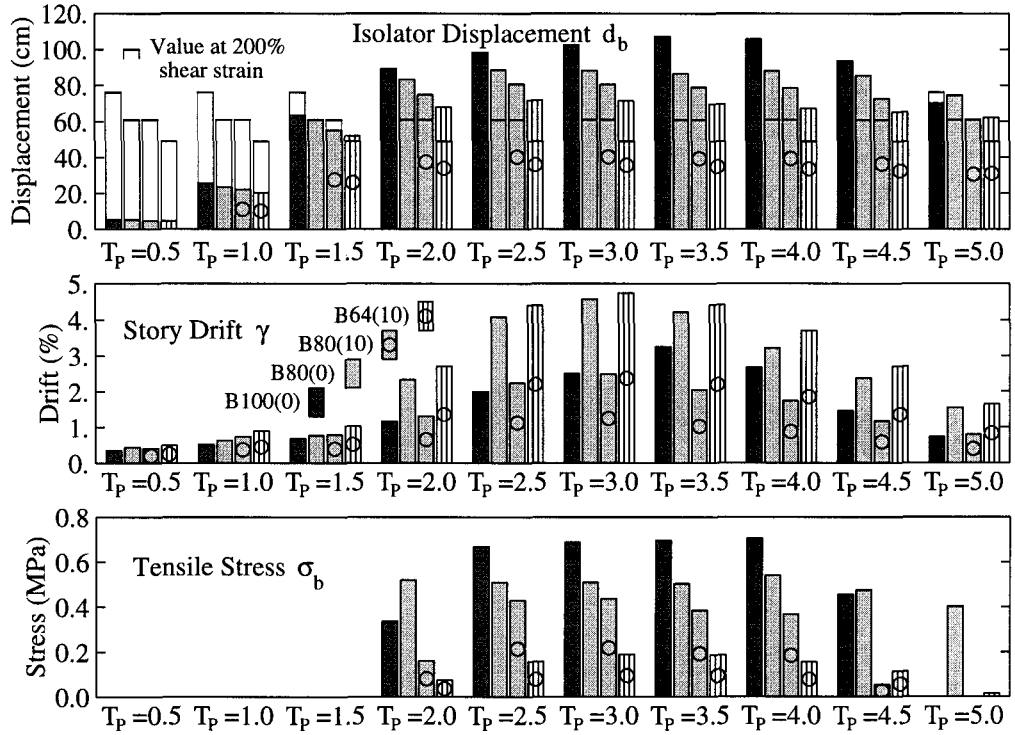

Figure 11. Peak responses of B100(0), B80(0), B80(10) and B64(10) to suite of pulses.

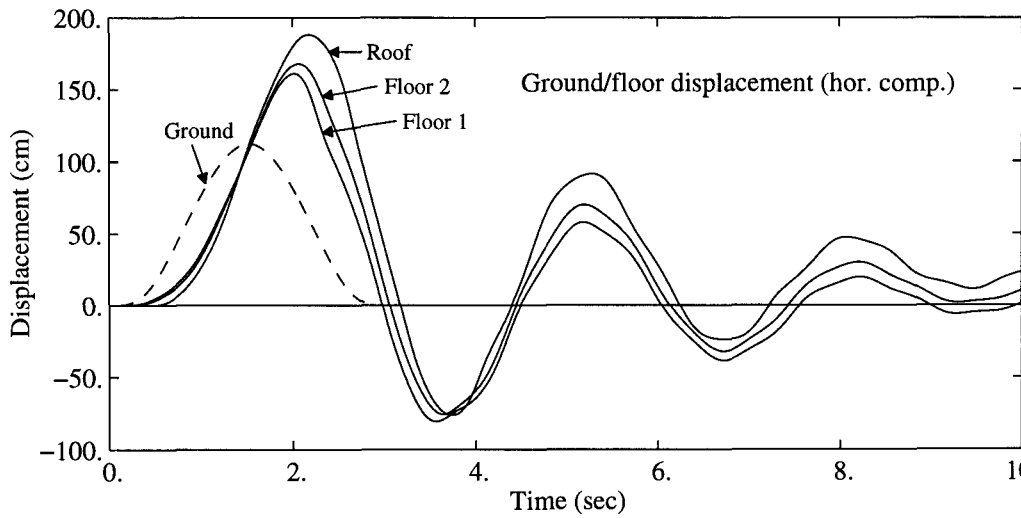

Figure 12. Horizontal displacement time histories for building B80(0) under the simple pulse with T_P = 3.0 seconds.

FURTHER STUDIES OF SUPPLEMENTAL DAMPING

The previous section indicates that if supplemental damping is added without lowering the design loads for the structure, it can be very effective in not only reducing the isolator displacement, but in improving structural performance. To investigate this in more depth, the previous design B80 is considered below with amounts of supplemental damping equal to 20% and 30% of critical [buildings denoted by B80(20) and B80(30), respectively].

Results are presented in Figure 13, and the data from Figure 9 for buildings B80(0) and B80(10) have been included. All four buildings have the same structure and isolation systems, just different amounts of supplemental damping. Response types included in Figure 13 are the same as those of Figure 9 except that total damper force $\mathcal{F}_d$ replaces the uplift stress. As expected, additional supplemental damping causes further reductions in the isolator displacement d_b. As far as improving structural response is concerned, supplemental damping seems to be most effective when it keeps the isolators from displacing far into their stiffening range. Note the significant reductions in story drift γ, plastic rotation θ_p and roof acceleration A_r between B80(0) and B80(10) for record H06 and between B80(0) and B80(20) for record C05.

The data of Figure 13 indicate that the optimal amount of supplemental damping is in the range of 10% to 20%. At the 20% value, the total supplemental damping force $\mathcal{F}_d$ nearly reaches 20% of the building dead weight W for the stronger records. Only the RRS record shows some penalty from the addition of supplemental damping in this amount, especially in roof acceleration. This is consistent with its response spectra in Figure 5 having a greater ratio of amplitude in the higher mode range of the building to the amplitude at the fundamental mode of 2.6 seconds. Overall, even the 30% supplemental damping level, which is actually superior for record C05, does not carry a significant penalty, and it produces a further reduction in isolator displacement. The true optimal amount of supplemental damping would be the one which best balances cost and performance factors.

Peak values of isolator displacement d_b and story drift γ for the suite of pulses appear in Figure 14. While there is a small penalty in story drift in the vicinity of $T_P = 1$ second due to the addition of supplemental damping, there is a substantial decrease in drift at higher periods as well as a significant reduction in isolator displacement. Responses with 20% supplemental damping are quite adequate, and a small further improvement is attained at the 30% level. Pending cost considerations, these results suggest 20% supplemental damping to be the optimal value.

DISCUSSION AND CONCLUSIONS

Because the *UBC* requires a dynamic design procedure using site-specific ground motion spectra when considering near-source effects, the results shown here are not sufficient to provide an assessment of the Code provisions, although they are relevant to this topic. At the least, they can be viewed as indicating the extent of measures needed to deal with strong near-source effects and the possible consequences when the ground displacements are large and rapid. For the eight actual earthquake records considered in this study, the $N_v = 1.6$ design level was found to achieve the Code's goal of essentially elastic behavior for the subject six-story building. However, the simulated record H06, intended to represent the most severe ground motion in the M_W6.7 Northridge earthquake, requires the $N_v = 2$ design level

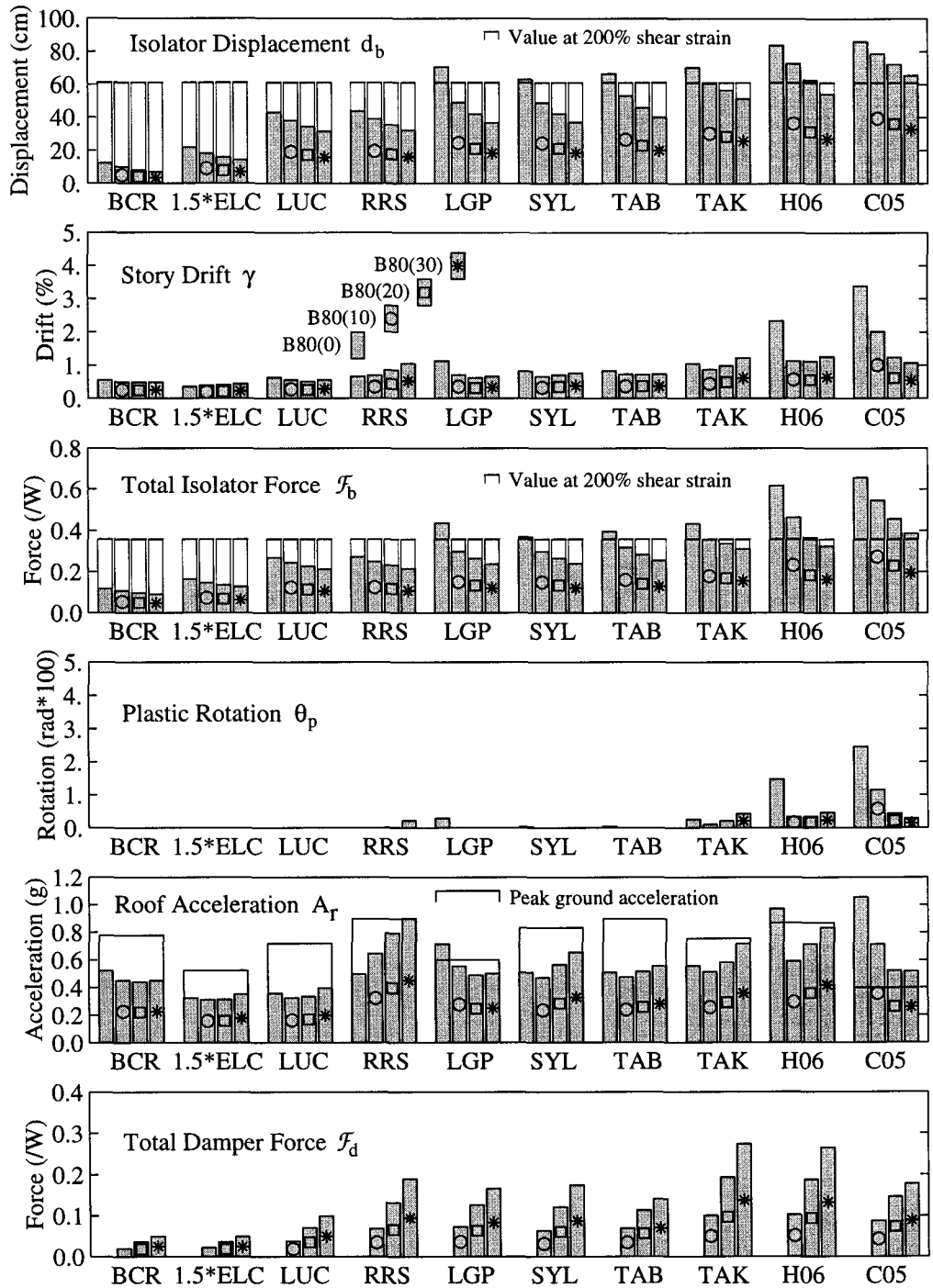

Figure 13. Peak responses of B80(0), B80(10), B80(20) and B80(30) to ten earthquake records.

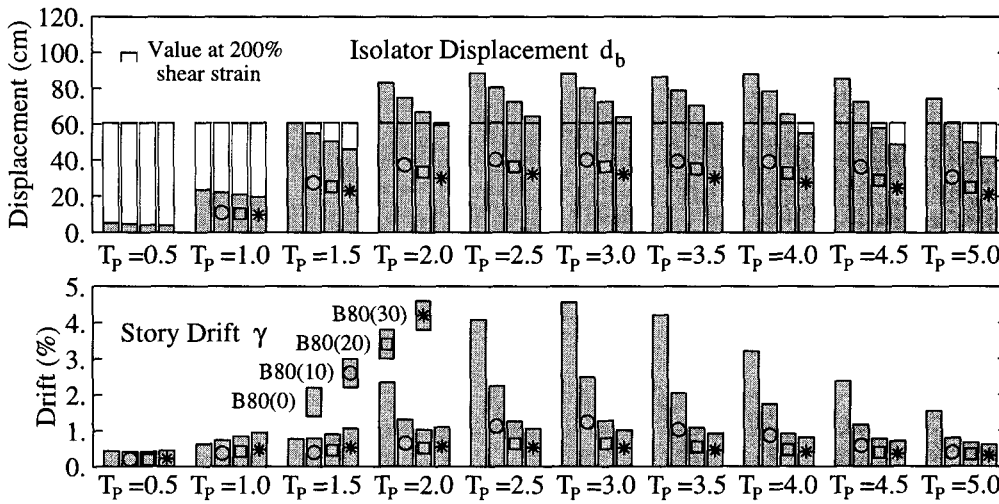

Figure 14. Peak responses of B80(0), B80(10), B80(20) and B80(30) to suite of pulses.

for similar performance, and even this design experiences plastic rotations of about 0.01 radians [building B80(10)] under the simulated record C05 from a hypothetical M_w7.0 thrust earthquake. In addition, a single ground displacement pulse of moderately large size, whose duration approximately matches the vibration period of the isolated building, can produce significantly greater response. As shown for the six-story building, a three-second pulse with 113 *cm* peak displacement and 129 *cm/sec* peak velocity causes story drift of about 2.5% for the N_V = 2 designs and nearly 5% for the N_V = 1.6 designs. Without supplemental isolator damping, corresponding values for isolator displacement are 102 *cm* and 88 *cm* for the two design levels, respectively. Obviously, the likelihood of such motions being produced needs to assessed through basic studies in earthquake mechanics.

Both the simulated motions H06 and C05 are from blind-thrust earthquakes, and the *1997 UBC* does not require that blind-thrust faults be used when determining the near-source factor (ICBO, 1997 and 1998). However, should an engineer wish to consider blind-thrust faults, it is relevant to note, according to *UBC* criteria, that the site and source characteristics for H06 would correspond to NV = 1.6 only and that the location for C05 is outside the near-source zones (Figure 15). As shown also in Figure 15, the *UBC*'s near-source zones inadequately cover the region of large ground displacements and velocities from the M_w7.0 blind-thrust earthquake simulation.

Strong ground motions can produce uplift tensile stresses in the bearings of taller isolated buildings, but these can be reduced to values thought to be reasonable by special design of the frame. In the example considered here, features which were incorporated include all frames being moment frames, interior frames being stiffer than exterior ones, and pinned connections used for all beams at exterior column locations above the first floor. The maximum tensile stress in a bearing seen in the studies presented here for the six-story building is 0.70 *MPa*.

Use of supplemental damping alongside the isolators effectively reduces the isolator displacement, greatly facilitating the design of the isolation system and other components which must accommodate this relative motion. If the strength of the structure is reduced when sup-

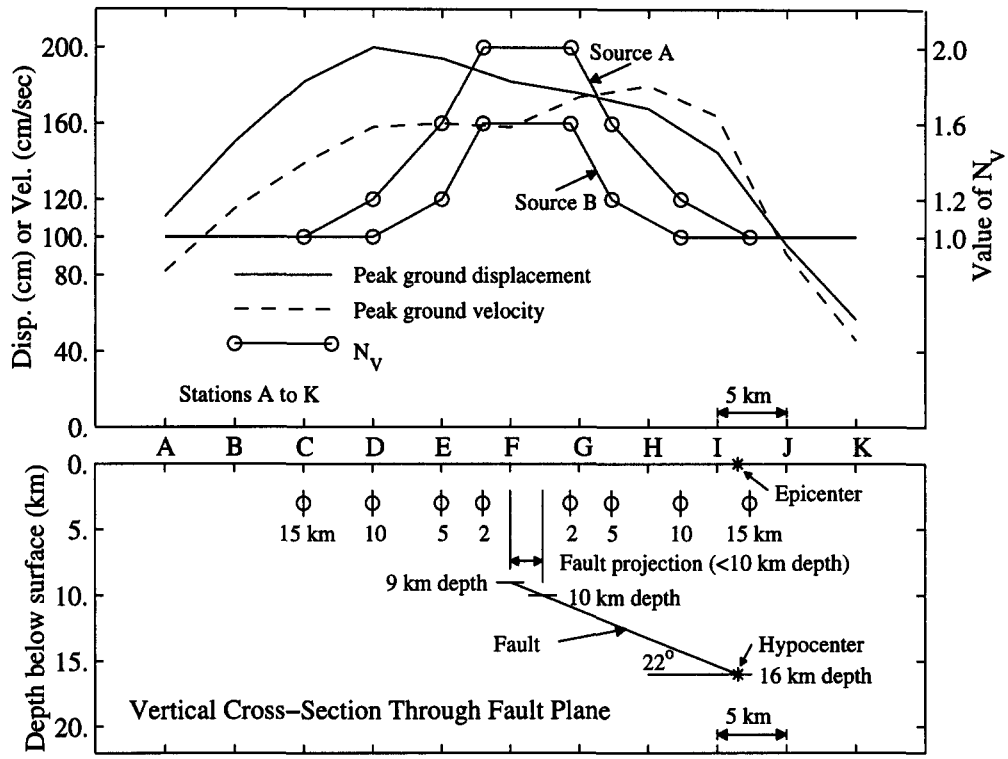

Figure 15. Top: Peak ground displacement and velocity from the simulated M_w7.0 blind-thrust earthquake from stations A to K along line 5 (see Figure 6). Also shown is the distribution of the UBC near-source factor N_V for Source A and Source B (ICBO, 1997). Bottom: Vertical cross-section through the fault plane showing the projection of the fault within 10 *km* of the ground surface and zones within 2 *km*, 5 *km*, 10 *km* and 15 *km* of the fault projection.

plemental damping is added, as allowed by the Code, then some small penalty in amount of story drift and yielding can be expected. On the other hand, when comparing identical buildings with and without supplemental damping, performance of the former is far superior. With 20% supplemental damping added to the building designed originally without such damping under N_V = 1.6, the largest isolator displacement and story drift seen in the present study are 73 *cm* and 1.3%, respectively. Both of these occur for the simple displacement pulse of three-second duration. The optimal amount of supplemental damping seems to be in the 10% to 20% range, pending cost analysis, which would put the total amount of damping associated with the isolation system in the 20% to 30% range. These results are consistent with a discussion (Hall, to appear) of concerns expressed by Kelly (1999) about the use of supplemental damping.

Without the addition of supplemental isolator damping, the larger isolator design displacements in the *1997 UBC* can make it difficult to achieve typical isolation periods (2 to 3 seconds) when rubber bearings are used. To withstand big lateral displacements, rubber bearings must be of large diameter, but this also makes them stiff. [The direct relation between the displacement capacity of an isolator and its stiffness is less applicable for sliding bearings, and

this is an advantage for such systems.] The smaller mass of shorter buildings compounds the problem, and a solution requires using fewer bearings either by increasing the column spacing or by transferring the load from more than one column to a single bearing. The example N_V=2 design considered in this paper employs very soft rubber to attain a 2.6-second isolation period. A building shorter than six stories would have required eliminating some of the bearings if the Code provisions were to be met without the use of supplemental damping.

Use of the large shear strain capability of rubber bearings, as done in this study and as advocated by Kelly (1997), is a departure from most past practice and has not been validated yet by sufficient realistic testing. Such testing should be done at full scale and should include application of vertical tensile and compressive load simultaneous with maximum shear. The benefit of rubber stiffening at large strains as a natural restraining device may be an improvement over sudden impact with a surrounding moat wall as examined by Hall et al. (1995), but it still significantly increases the shear transferred up into the superstructure and can cause large yielding excursions there.

REFERENCES

Asher, J. W., Young, R. P. and Ewing, R. D., 1996, Seismic isolation design of the San Bernardino County Medical Center replacement project, *The Structural Design of Tall Buildings*, **5**, 265-279.

International Conference of Building Officials, 1997, *Uniform Building Code*, Volume 2, Whittier, CA.

International Conference of Building Officials, 1998, *Maps of Known Active Fault Near-Source Zones in California and Adjacent Portions of Nevada*, Whittier, CA, February.

Hall, J. F., 1997, Seismic response of steel frame buildings to near-source ground motions, *Report No. EERL 97-05*, Caltech, Pasadena, CA.

Hall, J. F., Heaton, T. H., Halling, M. W., and Wald, D. J., 1995, Near-source ground motion and its effects on flexible buildings, *Earthquake Spectra*, **11**, 569-606, November.

Hall, J. F., to appear, Discussion of 'The role of damping in seismic isolation' by J. M. Kelly, *Earthquake Engineering and Structural Dynamics*.

Kasalanati, A. and Constantinou, M. C., 1999, Experimental study of bridge elastomeric and other isolation and energy dissipation systems with emphasis on uplift prevention and high velocity near-source seismic excitation, *Technical Report MCEER-99-0004*, University at Buffalo, State University of New York, Buffalo, NY.

Kelly, J. M., 1999, The role of damping in seismic isolation, *Earthquake Engineering and Structural Dynamics*, **28**, 3-20, January.

Kelly, J. M., 1997, *Earthquake-Resistant Design with Rubber*, Springer-Verlag, 2nd Edition.

Makris, N. and Chang, S.-P., 1998, Effect of damping mechanisms on the response of seismically isolated structures, *Report No. PEER-98/06*, Pacific Earthquake Engineering Research Center, University of California, Berkeley, CA.

Ryan, K. and Hall, J. F., 1998, Aspects of building response to near-source ground motions, *Proceedings of Structural Engineering World Congress*, San Francisco.

Seleemah, A. A. and Constantinou, M. C., 1997, Investigation of seismic response of buildings with linear and nonlinear fluid viscous dampers, *Technical Report MCEER-97-0004*, University at Buffalo, State University of New York, Buffalo, NY.